

© Williams & Wilkins 1997. All Rights Reserved.

Volume 29(3), March 1997, pp 313-319

Rat tendon morphologic and functional changes resulting from soft tissue mobilization

[Clinical Sciences: Clinically Relevant]

DAVIDSON, CRAIG J.; GANION, LARRY R.; GEHLEN, GALE M.; VERHOESTRA, BETH; ROEPKE, JANET E.; SEVIER, THOMAS L.

Ball Memorial Hospital, Muncie, IN 47304; Department of Physiology, Ball State University, Muncie, IN 47306; and Biomechanics Laboratory, Ball State University, Muncie, IN 47306

Address for correspondence: Gale Gehlsen, Biomechanics Laboratory, PL202, School of Physical Education, Ball State University, Muncie, IN 47306. E-mail: OOGMGEHLEN@BSUVC.BSU.EDU.

ABSTRACT

Augmented Soft Tissue Mobilization (ASTM) is a new non-invasive soft tissue mobilization technique which has been used successfully to treat a variety of musculoskeletal disorders. The purpose of this study was to determine the effects of ASTM therapy on the morphological and functional characteristics of enzyme induced injured rat Achilles tendons. Four groups of five rats were allocated as follows: (A) control, (B) tendinitis, (C) tendinitis plus ASTM, and (D) ASTM alone. Collagenase injury was induced, and the surgical site was allowed to heal for 3 wk. ASTM was performed on the Achilles tendon of groups C and D for 3 min on postoperative days 21, 25, 29, and 33 for a total of four treatments. Gait data were gathered prior to each treatment. The Achilles tendons of each group were harvested 1 wk after the last treatment. Specimens were prepared for light and electron microscopy, and immunostaining for type I and type III collagen and fibronectin was performed. Light microscopy showed increased fibroblast proliferation in the tendinitis plus ASTM treatment group. Although healing in rats may not translate directly to healing in humans, the findings of this study suggest that ASTM may promote healing *via* increased fibroblast recruitment.

Massage remains as one of the oldest forms of therapy for many musculoskeletal disorders. Several forms of massage or soft tissue mobilization techniques have been developed and used for the treatment of chronic tendon inflammatory conditions, such as lateral epicondylitis, patellar tendinitis, and rotator cuff tendinitis (4). How soft tissue mobilization specifically functions to foster improved tendon action is not clearly understood. According to Norris (21), the purpose of frictional massage is to promote a local hyperemia, massage analgesia, and reduction of adherent scar tissue. In addition, Prentice (24) has hypothesized that frictional massage may facilitate tendon healing by augmenting the inflammatory process to completion so the later stages of healing can occur.

Much of what is known about tendon healing has been gained from animal studies involving the transection of tendons (9,12,25). Tendon healing of acute injuries occurs in three stages: inflammation, proliferation, and remodeling (13). During the inflammatory stage, blood platelets and fibrin fill the wound and fibroblasts and phagocytic cells migrate to the injured site. The fibroblasts begin to produce fibronectin. In the proliferative stage, fibroblasts increase in number and synthesize collagen. The remodeling or maturation stage involves a reduction in cellularity and realignment of collagen fibers. Also collagen production shifts from immature, Type III collagen, to mature, Type I collagen, and fibronectin decreases. It is assumed that this repair process is similar and functions in the healing of chronic tendinitis (13).

Recently we have had success treating tendinitis patients with a therapeutic technique called Augmented Soft Tissue Mobilization (ASTM). ASTM is a modification of traditional

soft tissue mobilization and uses specifically designed solid instruments. These instruments, rather than hands and fingers of the therapist, are used to provide the contact mobilization force in the treatment of tendinitis. We theorize that the ASTM therapeutic technique allows a therapist to introduce more effectively a controlled amount of microtrauma into an area of excessive scar and/or soft tissue fibrosis. The response of the tendon to this microtrauma could involve augmentation of the healing process. The purpose of this study was to characterize morphologic and functional changes in the rat Achilles tendon following enzyme induced injury with collagenase and subsequent ASTM therapy. Because connective tissue natively contains collagen and the levels of collagenase rise after injury, the direct injection of collagenase provides a good model of chronic tendon inflammation (14,27). From gait analyses and microscopic studies, we describe functional, as well as structural and cellular, changes presumably affected by ASTM.

METHODS

Animals. Male Sprague-Dawley rats weighing between 225 and 263 g (27 wk old) were used in this study. The animals were housed five per standard rat cage and fed rat chow and water *ad libitum*. The animals were randomly assigned to one of four groups with five animals per group: control (A), tendinitis (B), tendinitis plus ASTM (C), and ASTM alone (D). The study was approved by The Ball State University Animal Care and Use Committee.

Achilles tendon injury. The Achilles tendons of animals in Groups B and C were injected with collagenase to induce tendinitis. Prior to the injection, the animals were anesthetized intramuscularly with a cocktail solution of Ketamine (35 mg·ml⁻¹) and xylazine (0.42 mg·ml⁻¹) at a dosage of 0.14 cc·100 g⁻¹ body mass. Next the hair overlying the left Achilles tendon was removed with a topical depilatory agent. After the skin was cleaned, a longitudinal incision was made slightly medial to the visible outline of the tendon. With a blunt dissection, the tendon was exposed distally near the calcaneal insertion. Under direct visualization, 30 ul of collagenase (10 mg·ml⁻¹) was injected into the tendon near the bone tendon junction. The incision was closed with several simple sutures of 5-0 ethilon and a single 0.2 cc dose of bicillin (300,000 U·ml⁻¹) was administered intramuscularly for prophylaxis against infection. The surgical site was allowed to heal for 3 wk before treatment.

Augmented soft tissue mobilization. Animals in Groups C and D underwent augmented soft tissue mobilization. An aluminum instrument was made specifically for applying ASTM to the Achilles tendon. To administer ASTM, animals were anesthetized *via* inhalation with metaphane and placed in a supine position with the left rear foot elevated for access to the Achilles tendon. Considerable pressure was applied to the tendon, but care was taken not to break the overlying skin. The tendon was massaged in a longitudinal plane, moving distal to proximal and proximal to distal along the length of the tendon. ASTM was performed on the Achilles tendon of Groups C and D for 3 min on postoperative days 21, 25, 29, and 33 for a total of four treatments.

Gait analysis. All animals in this study were subjected to gait analysis. For this purpose, a modified small motorized treadmill with a 23× 40 cm enclosed alley with clear plastic sides was used. The treadmill speed was 22 cm·s⁻¹. A Panasonic digital 5000 video camera was used to record the movements of each animal during treadmill testing. The camera was positioned perpendicular to the treadmill. Black ink joint markers were placed on shaven skin of the left hind limb (greater trochanter, knee joint center, lateral malleolus, fifth metatarsal, and fifth toe). The video data was analyzed with the aid of a Peak 5, video and analog motion measurement system (Peak Performance Technologies, Inc., Englewood, CO). The video sampling rate was 60 Hz. The following dependent variables were identified from the video: stride length, stride frequency,

and hip, knee, and ankle angular displacement. The running patterns of each group (A-D) were recorded prior to surgery and 1 d prior to ASTM treatments.

Light microscopy. Ten days after the last ASTM treatment, the tendons were prepared for light microscopy to detect possible structural changes such as collagen fiber alignment, number of fibroblasts, and presence of inflammatory cells. The animals were sacrificed and the tendon harvested by excision of the lower limb superior to the knee joint. The foot and fur were removed from the excised limb. The limb was then fixed overnight in 10% buffered formalin and subsequently decalcified in two changes of 1 N HCL for 6 d. The specimen was then bisected along the midsagittal plane. The resultant specimens were then dehydrated through a graded alcohol series and xylene and embedded in paraffin. Tissue sections were cut at 4 μ , stained with hematoxylin, counterstained with eosin, and mounted and observed with a bright field microscope.

Fibroblast numbers were assessed by light microscopy. Fibroblast counts were performed on five tendon specimens from each group. Counts from 10 random, 450X microscopic fields were recorded.

Electron microscopy. To assess possible changes in the fine structure of fibroblast endoplasmic reticulum through routine electron microscope study, the Achilles tendon was cut free from the paraffin blocks with a razor blade. The tendon was then placed in xylene to remove the paraffin, rehydrated, cut into 1 mm³ blocks, postfixed in 1% osmium tetroxide in 0.1 M cacodylate buffer, dehydrated in a graded series of ethanols, and embedded in LX-112 (Ladd Research Industries, Burlington, VT). After polymerization at 60°C for 24 h, the cured blocks were trimmed and 1 μ m thick sections were cut with glass knives on a LKB ultratome. The thick sections were stained with toluidine blue and surveyed with the bright field microscope. Favorable blocks were retrimmed and 800-900 nm ultrathin sections obtained with a diamond knife. The thin sections were picked up on 200 mesh copper grids, stained with 2% uranyl acetate, counterstained with lead citrate, and examined with a Hitachi H-600 transmission electron microscope.

Immunoelectron microscopy. One Achilles tendon from each experimental group was prepared for immunolabeling. The excised tendons were fixed in a cocktail of 1% glutaraldehyde and 1.5% paraformaldehyde in 0.1 M cacodylate buffer for 1 h at room temperature. After cutting and dehydration, the 1 mm³ tissue blocks were embedded in Unicryl (Goldmark Biologicals). Polymerization was completed at 50°C for 48 h. Thin sections were cut and picked up on 200 mesh nickel grids.

Sections were then stained for Type I or Type II collagen or fibronectin as follows. First, the thin sections were incubated in 0.2% bovine serum albumin for 15 min at 37°C and then in a 1:20 dilution of rabbit anti-human Type I or Type II collagen (Sanbio, Am Uden, The Netherlands) or a 1:3000 dilution of rabbit anti-human fibronectin (Sigma Immunochemicals, St. Louis, MO) for 2 h at room temperature. Negative controls were incubated in 0.1 M cacodylate buffer. After a brief rinse in cacodylate buffer, the sections were incubated overnight at 4°C in a 1:50 dilution of goat anti-rabbit immunoglobulin coupled with 10 nm colloidal gold (Dako Corp., Carpinteria, CA). Next, sections were rinsed in cacodylate buffer and postfixed in 3% glutaraldehyde for 1 h at room temperature. After a final rinse in distilled water, the sections were stained with 2% uranyl acetate and lead citrate and viewed with the transmission electron microscope.

Statistical analysis. The mean fibroblast count for each group was calculated and the significant difference between groups was determined by Kruskal-Wallis oneway

ANOVA and Newman Keuls *post-hoc* procedures. For all gait analysis measures (i.e., stride length, stride frequency, and ankle angular displacement), the influence of treatment and treatment session was examined by two-way ANOVA with repeated measures. Newman-Keuls *post-hoc* tests were applied where appropriate. An alpha value of 0.05 was used for analyses.

RESULTS

Light microscope. With the light microscope (Figs. 1 and 2), structural differences were observed in the tendons of the four groups. In group A, the collagen fibers were aligned in parallel and few fibroblasts were observed. The tendons of group B exhibited disrupted and randomly arranged collagen fibers and numerous fibroblasts. The collagen fibers of Group C tendons were also misaligned. In addition, Group C tendons had a great abundance of fibroblasts. Groups D tendons manifested parallel aligned fibers and occasional areas with increased numbers of fibroblasts.

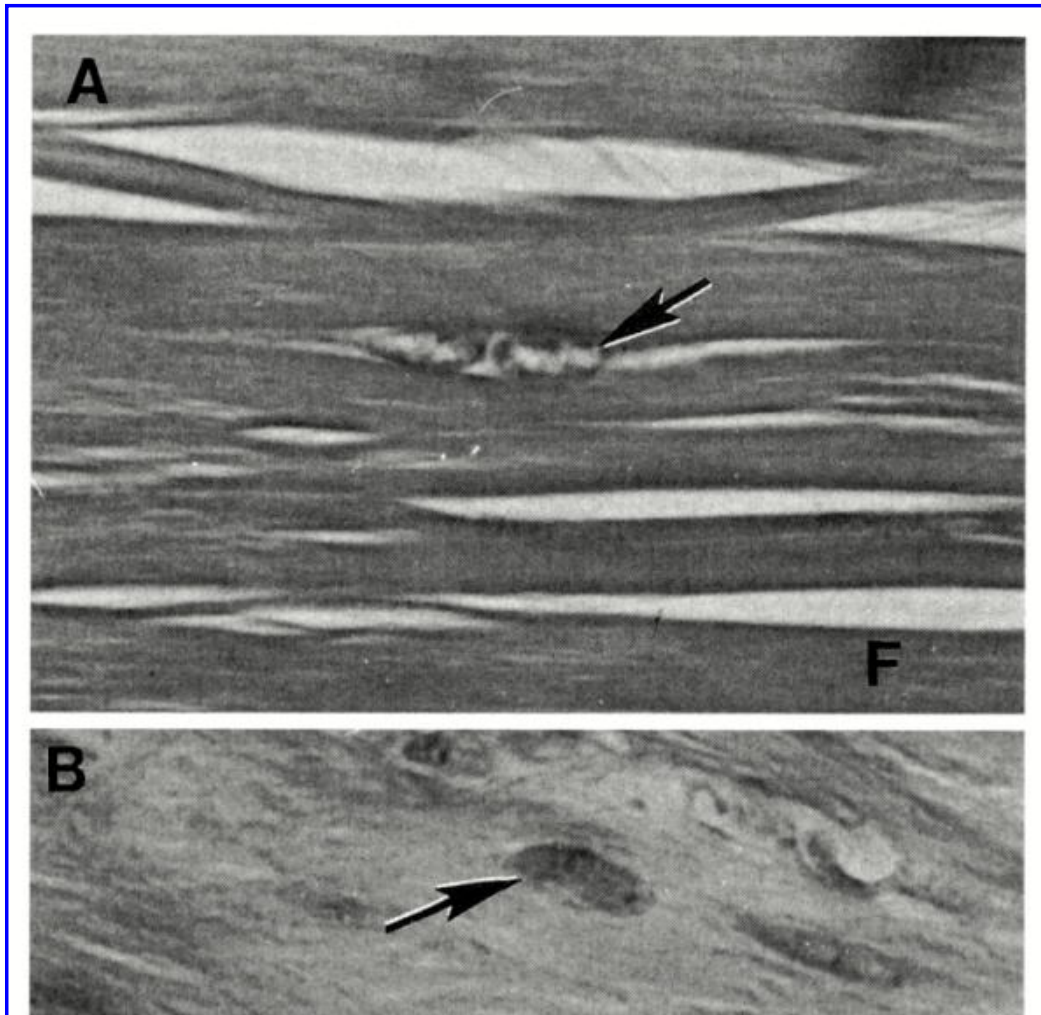




Figure 1-Light photomicrographs illustrating tendon morphology of A(photo A) and Group B (photo B). Note the increased number of fibroblasts(arrows) and misaligned collagen fibers in Group B. Collagen fibers, F; $\times 400$.

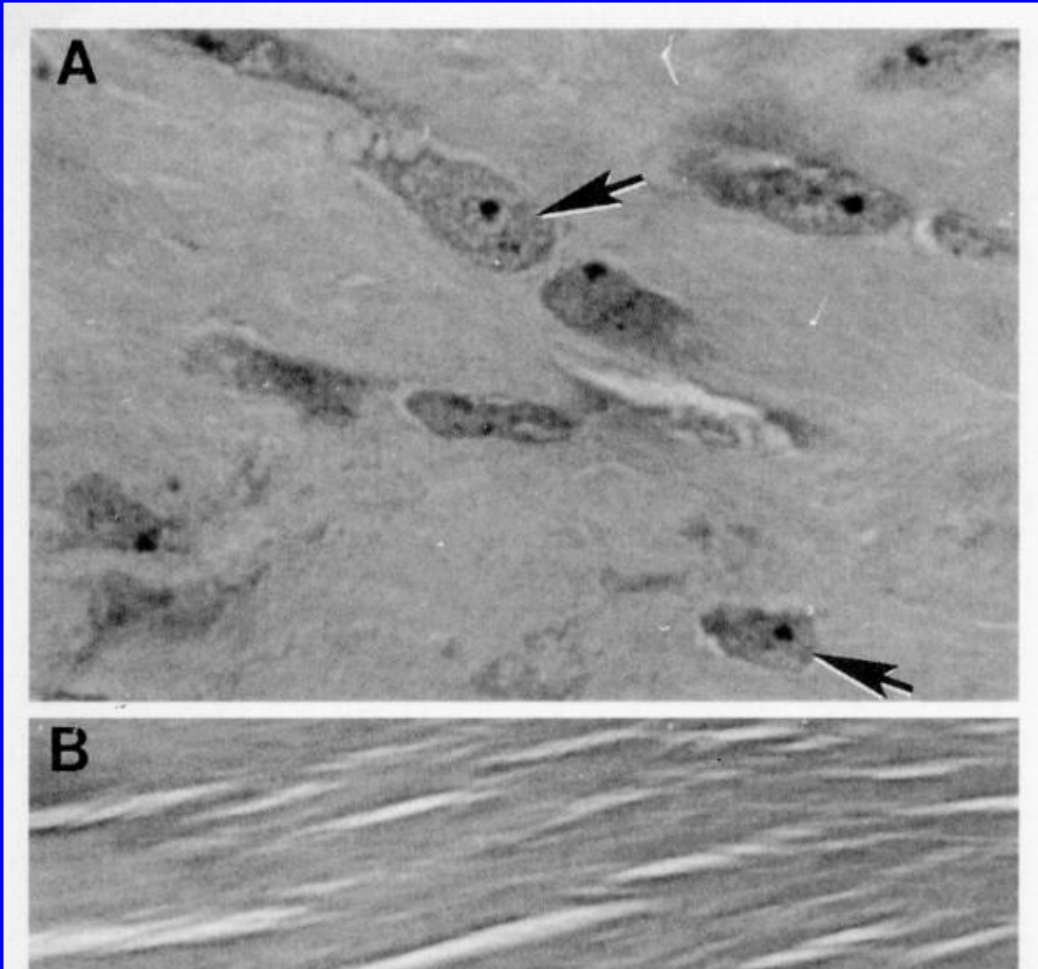




Figure 2-Light photomicrographs illustrating tendon morphology of Group C (photo A) and Group D (photo B). Numerous fibroblasts are evident in Group C. The collagen fibers are misaligned in Group C and parallel in Group D. Fibroblasts (arrows); Collagen fibers, F; $\times 400$.

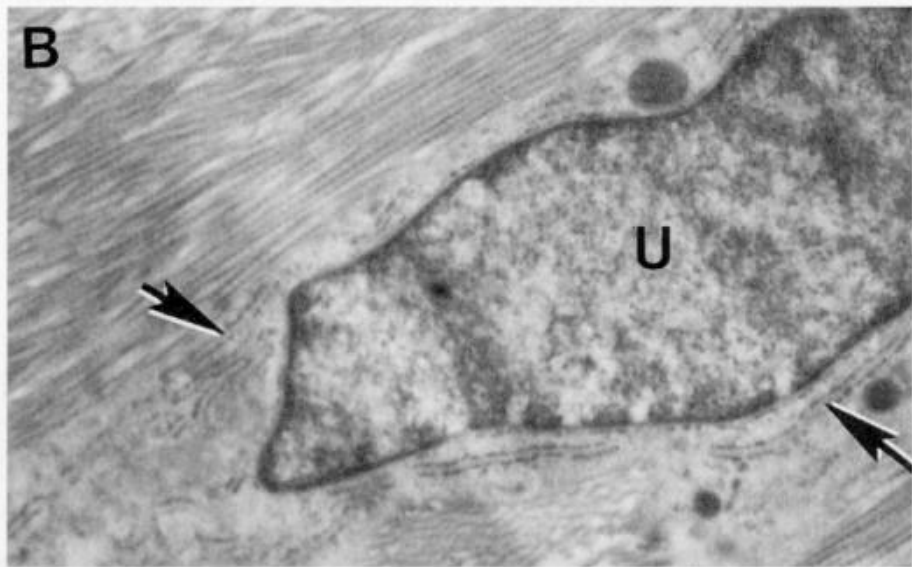
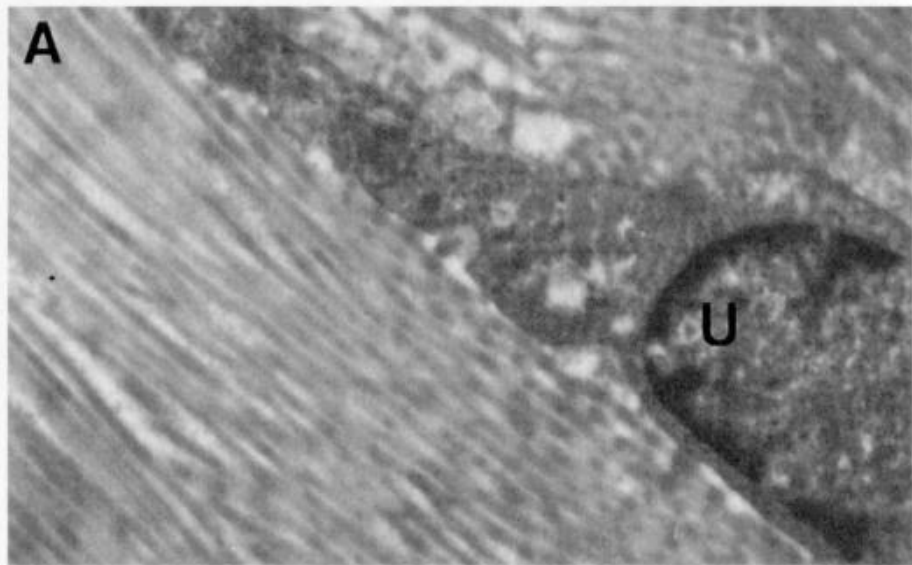
Fibroblast counts. Fibroblast counts were performed to more accurately assess fibroblast numbers. Table 1 describes the fibroblast count expressed as a mean of five specimens. For each specimen, ten microscopic fields at 450X were counted. ANOVA indicated a significant difference ($P < 0.00$) between groups with three degrees of freedom ($H = 26.9$). *Post-hoc* analysis indicated a significant difference ($P < 0.05$) between Group C fibroblast counts and all other groups' fibroblast counts. Significant differences were also noted between groups B and A and groups B and D. No significant difference occurred between groups A and D.

Subject Group	Fibroblast Count (mean)
A	3 ± 3
B	10 ± 7
C	$15 \pm 11^*$
D	4 ± 2

* Significant difference noted between group C and all other groups.

TABLE 1. Fibroblast counts expressed as mean of five specimens. For each specimen, 10 microscopic fields at 450 \times were counted.

Electron microscopy. To determine whether ultrastructural alterations occurred within the fibroblasts of the various groups, the tendons were examined with the transmission electron microscope. One of the structural features of fibroblasts actively synthesizing collagen is the presence of rough endoplasmic reticulum within the cytoplasm. As shown in Figure 2, the fibroblasts of the control tendons appeared normal and displayed few, if any, profiles of rough endoplasmic reticulum. Although not illustrated, a few profiles of rough endoplasmic reticulum were observed in the fibroblasts of Group B. The rough endoplasmic reticulum was highly developed in the fibroblasts of Group C (Fig. 3). The tendons of Group D also displayed numerous profiles of rough endoplasmic reticulum.



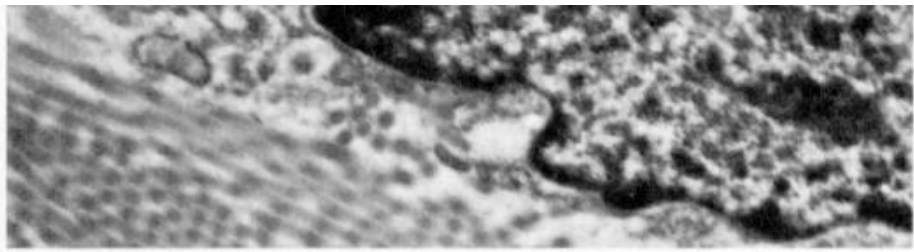
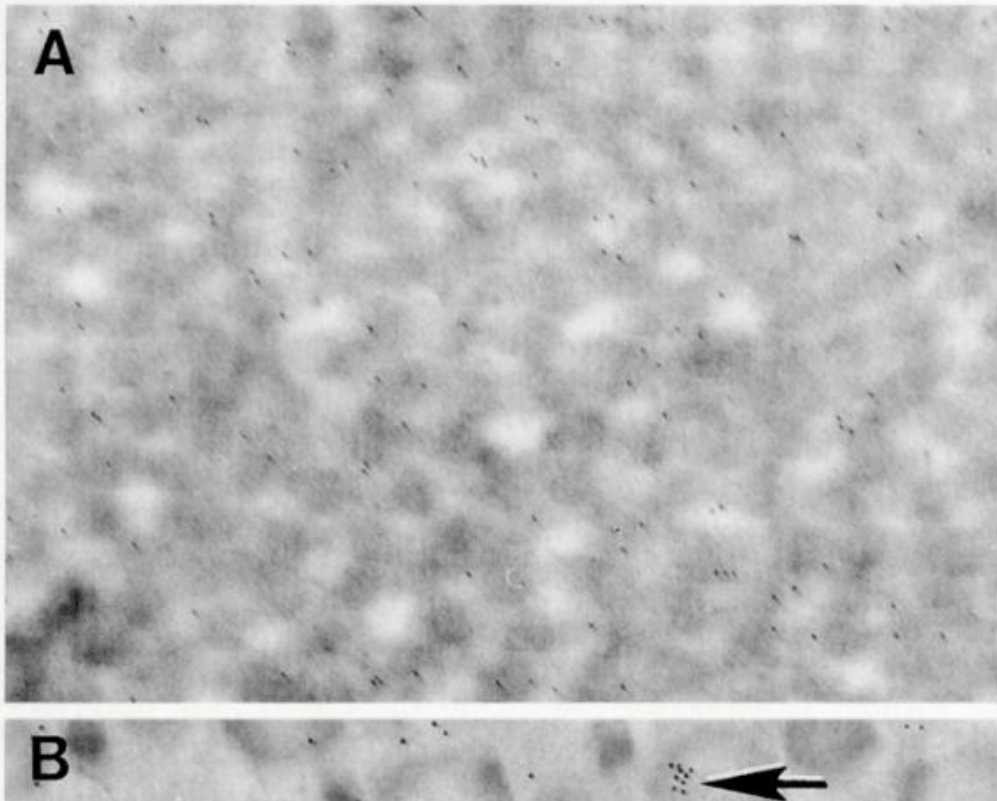


Figure 3-Electron micrographs of fibroblasts representative of Group A tendons (photo A), Group C tendons (photo B), and Group D tendons (photo C). Note the abundance of rough endoplasmic reticulum (arrows) in fibroblasts of Group C and Group D. Nucleus, U; $\times 10,000$, a; $\times 12,000$, B and C.

Immunoelectron microscopy. Immunolabeling with colloidal gold was performed to assess the synthesis of Type I and Type III collagen as well as the presence of fibronectin in tendons of the control and treatment groups. The tendons of all four groups stained diffusely with antibodies to Type I and Type III collagen. In all cases, the colloidal gold staining of Type I and Type III collagen appeared to be of equal intensity. While the labeling of Type III collagen was diffuse in Group C, numerous foci of intense staining were evident (Fig. 4). As illustrated in Figure 5, the tendons of Group C, unlike Group A, stained appreciably with fibronectin antibodies. Little fibronectin labeling occurred in the tendons of Group B, but those of group D stained strongly positive for fibronectin.



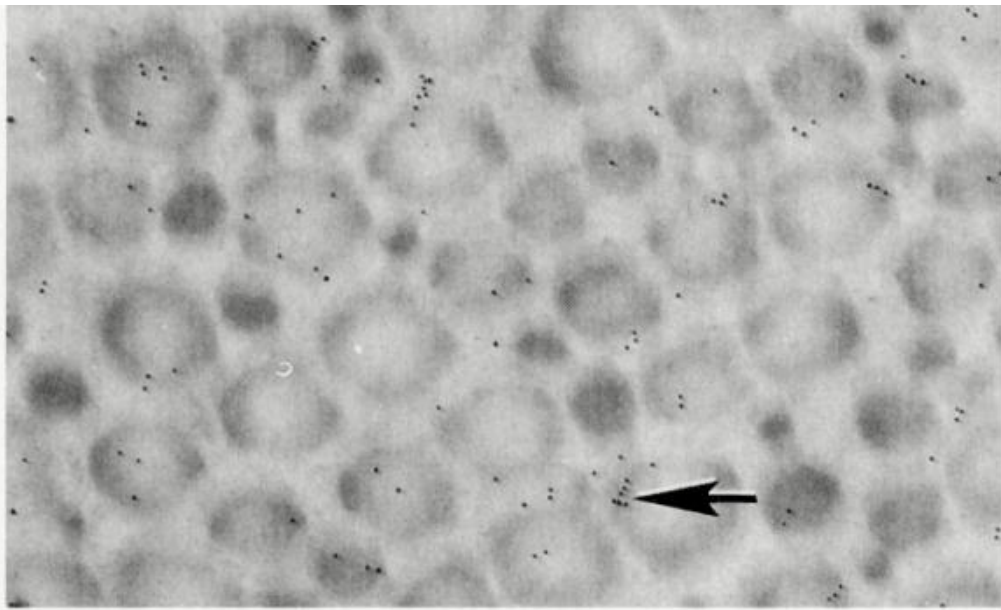


Figure 4-Electron micrographs showing immunolabeling of Type III collagen. Both Group A (photo A) and Group C (photo B) tendons are diffusely labeled. Group C tendons display foci of intense staining (arrows)

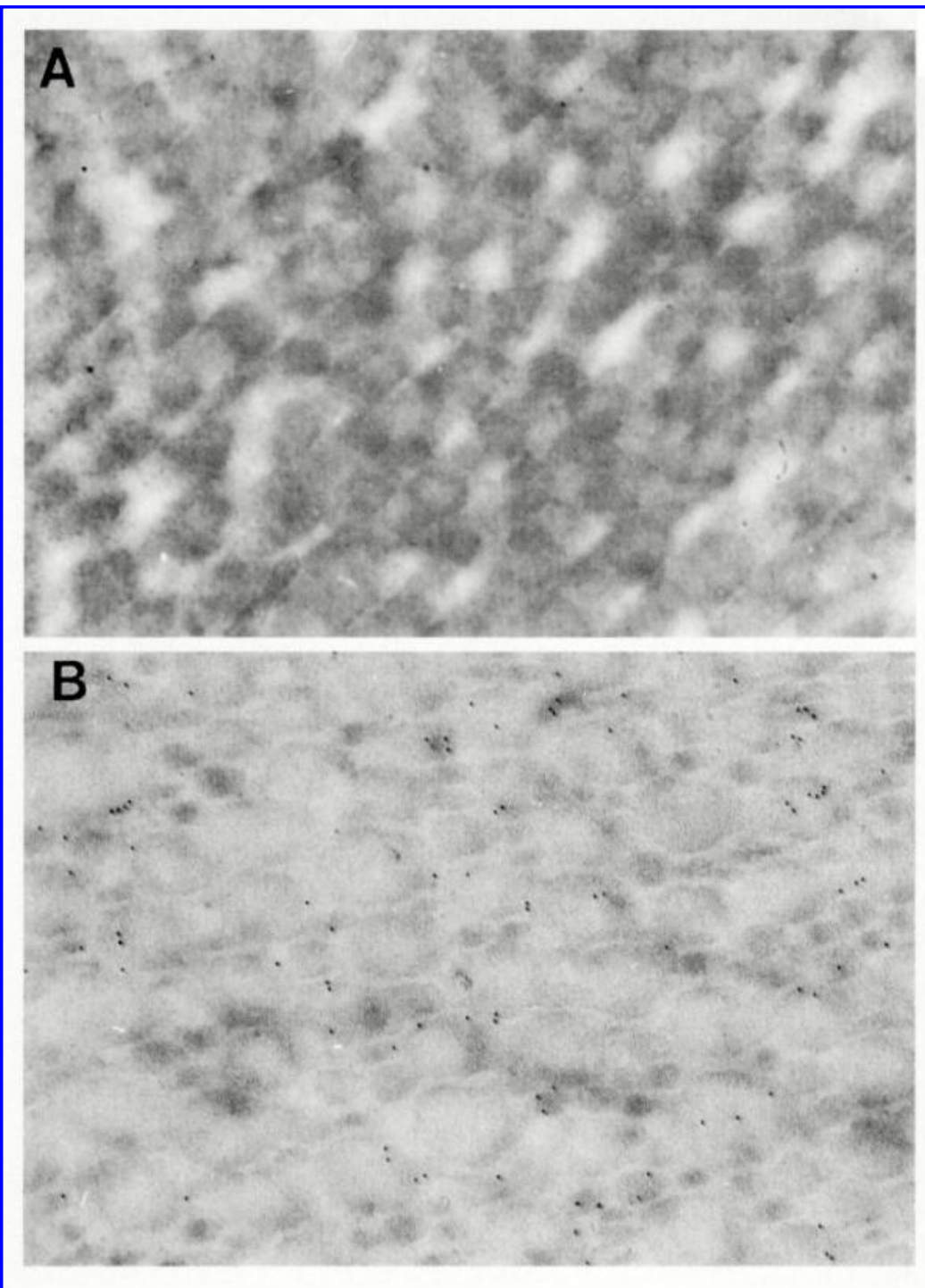


Figure 5-Electron micrographs of Group A (photo A) and Group C(photo B) tendons immunostained for fibronectin. Note staining of Group C tendon; x 30,000.

Gait analyses. Figure 6 presents the stride length and stride frequency values for each observation. A significant difference between post surgery day 21 and the final observation was indicated for only animal Group C's stride length and stride frequency. The mean stride length difference was 2.3 cm, and the mean stride frequency difference was 1.6 Hz.

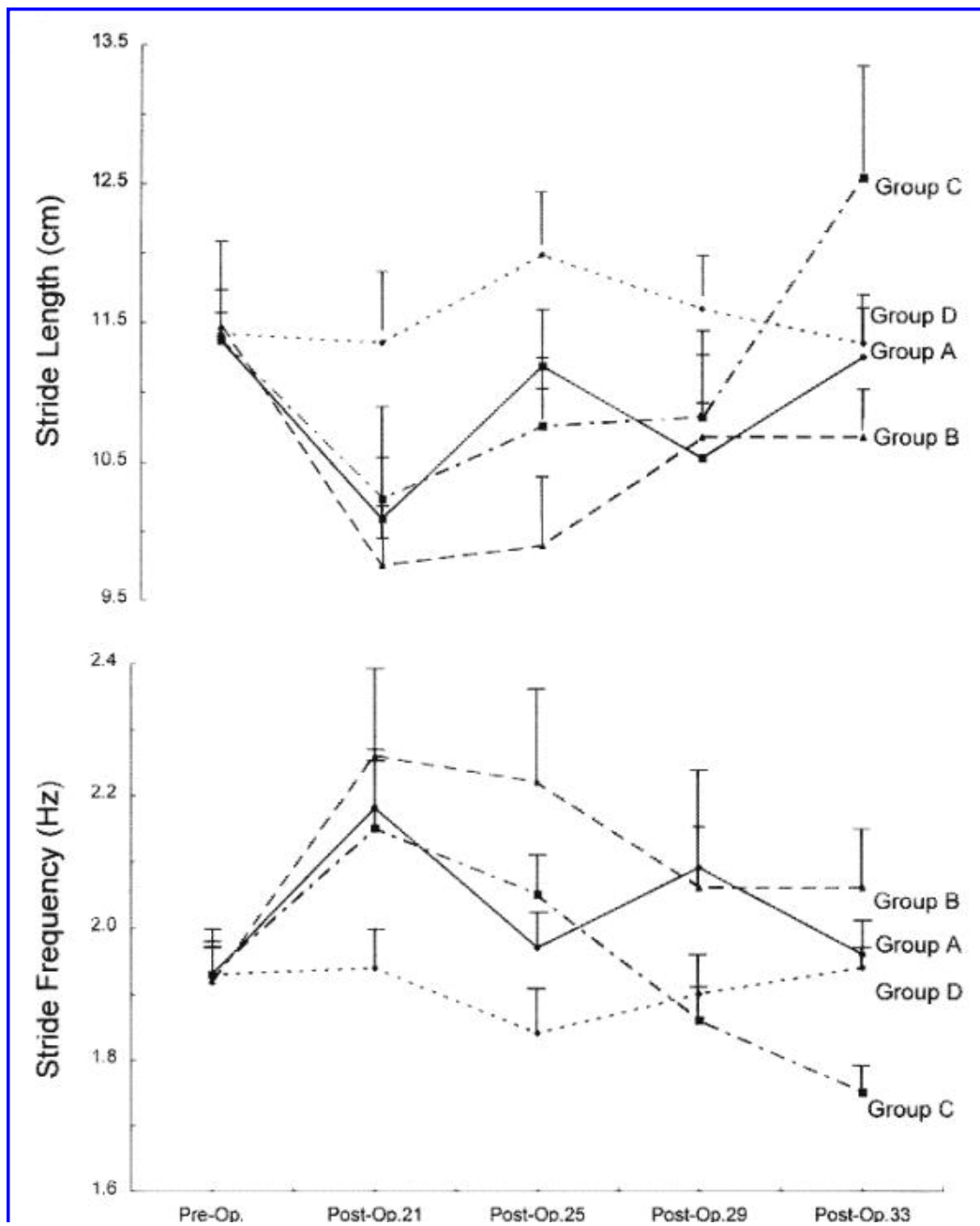


Figure 6-Stride length and stride frequency mean values for the four treatment groups prior to their surgical operation and from 21 to 33 d after surgery.

Ankle, knee, and hip joint angular kinematics were determined. In Groups A and D the mean range of motion varied only 2-3°. The range of motion values in Groups B and C decreased as much as 25° and then improved with therapy and time, with only the knee joint range of motion values reaching a statistically significant level. Over the course of this study, knee joint range of motion after injection increased 24.6 and 21.1° in Groups B and C, respectively.

DISCUSSION

The use of physical agents and procedures to facilitate healing of tendon injuries has been studied on numerous occasions (23-27). For example, there is growing evidence of the therapeutic effectiveness of ultrasound (7,11,22) and galvanic stimulation (3,19,20,23) in promoting tissue and tendon repair. The results of the present study not only demonstrate improved limb function following ASTM treatment, but also suggest ASTM may facilitate tendon healing by the recruitment and activation of fibroblasts.

The gait results presented here appear to support the morphological data in that only the animals in Group C significantly improved their running performance after injury. The gait data further indicate that both injured groups appeared to improve with time. However, the ASTM treatment animals (Group C) appeared to return to their original pattern within the time frame of this study.

One of the reported features of tendon healing is the proliferation of fibroblasts. This study clearly demonstrated a significant increase in fibroblast number in two of the experimental groups. Similar to other studies (27,28), we also observed the occurrence of an increase in fibroblast numbers in tendons following collagenase injury (Group B). Interestingly, the largest significant increase in the number of fibroblasts was evident in the collagenase-ASTM treated tendons of Group C. There was no significant difference in fibroblasts number between Groups A and D. These results suggest that ASTM of the injured tendons may aid in the healing process. In this regard, it has been hypothesized that massage may augment healing (24).

The results of this study also suggest that ASTM may facilitate the activation of fibroblasts. Numerous EM studies have shown that following tendon transection the quiescent fibroblasts become activated (9,11,12,25). Activated fibroblasts typically exhibit prominent nucleoli, numerous ribosomes, Golgi, and an abundance of rough endoplasmic reticulum (9,29). The cisternae of the rough endoplasmic reticulum is often described as being distended (9,25,29). Such cellular features within fibroblasts are now known to be associated with collagen synthesis (9,29). Fibroblast activation is an important and initial step in tendon healing. In the present study, activated fibroblasts with well developed rough endoplasmic reticulum were observed in all three experimental Groups and not in the control group. In Groups B and C fibroblast activation probably occurred in response to injury caused by the injection of collagenase. Of interest is the presence of activated fibroblasts in tendons of animals subjected only to ASTM (Group D). The fibroblasts of this Group, as well as those of Group C, displayed an abundance of rough endoplasmic reticulum. These observations imply that ASTM may initiate fibroblast activation, which eventually leads to collagen synthesis.

The formation and maturation of collagen during wound healing has been the topic of numerous studies. Type III collagen, normally found in embryonic tissues, reportedly is

synthesized early in the repair response to tissue injury and later during maturation is replaced by Type I collagen (2,10). Information on the distribution of Type I and Type III collagen during tendon repair is limited. A study by Williams et al. (28) used an equine model to examine the localization of Type I and Type III collagen in tendons after collagenase induced injury. The tendons 1 wk after injury were stained with antibodies to both Type I and Type III collagen. One wk later, Type I collagen staining reportedly became more prominent and by 14 wk Type III collagen staining appeared less pronounced. Further, widespread Type III collagen staining was seen in the control tendons. In the present study all four tendon groups stained diffusely with antibodies to Type I and Type III collagen, and no difference in staining intensity was observed. However, numerous foci of intense Type III collagen staining were seen in the injured tendons of the ASTM treated animals (Group C). These foci probably represent localized areas of newly synthesized type III collagen.

Fibronectin, synthesized by fibroblasts and endothelial cells (5,6), is a noncollagenous glycoprotein that acts as an adhesive molecule to integrate the extracellular matrix and bind collagen (17). During the initial tissue response to injury, fibronectin synthesis increases and later declines as healing proceeds (15,16). Williams et al. (27), studying equine tendon healing in ponies, noted widespread fibronectin staining of matrix 1 wk after induced collagenase injury and later observed a reduced intensity of fibronectin staining. We also observed fibronectin staining in tendons after collagenase induced injury (Group B). In addition, fibronectin staining was exhibited by collagenase injured tendons treated with ASTM Group C. Interestingly, tendons only subjected to ASTM (treatment Group D) also exhibited fibronectin staining.

The normal initial response of tissue to injury is inflammation with the appearance of numerous mononuclear blood cells and lymphocytes at the injured site (18). In the present study, we did not observe any inflammatory cells. This failure to observe such an inflammatory reaction may be related to our choice of experimental animal and method of induced injury. The traditional model of tendinitis is established *via* total or partial transection of the tendon. This model has been explored in a variety of animals, including the rat, and an acute inflammatory reaction is seen (8,9,25). While the injection of collagenase into tendons has been reported to trigger an acute inflammatory response in horses and ponies (26-28), it apparently does not elicit one in the rat. In a related study, Zamora et al. (29) cut tendons of synergist muscles to study the effects of overload on the myotendinous junctions of the rat and noted tendon collagen bundle disruption, fibroblast activation, and an absence of inflammatory cells.

The hallmark of tendon injury is collagen fiber disruption and misalignment (11,25,27); this hallmark was exhibited in this study. The final phase of tendon repair entails the realignment of collagen fibers. This maturation phase typically requires 2 or 3 months to accomplish (17) and was not evident in our study. The factors responsible for this realignment are unclear, but probably involve mechanical forces such as tension and compression resulting from the contraction of associated muscles (1). As evident by the gait analysis data, ASTM appeared to promote healing and earlier recovery of limb function following collagenase injury. With an earlier restoration of limb function, it seems likely that mechanical force would act sooner to promote collagen fiber realignment and thus hasten the completion of tendon repair.

REFERENCES

1. Barlow, Y. and J. Willoughby. Pathophysiology of soft tissue repair. *Br. Med. Bull.* 48:698-711, 1992. [IUCAT Link A-to-Z Link Bibliographic Links](#) [Context Link]
2. Barnes, M. J., L. Morton, R. Bennett, A. Bailey, and T. Simms. Presence of Type III collagen in guinea-pig dermal scar. *Biochem J.* 157:263-266, 1976. [IUCAT Link A-to-Z Link Full Text Bibliographic Links](#) [Context Link]

3. Bourguignon, G. J. and L. Y. W. Bourguignon. Electrical stimulation of protein and DNA synthesis in human fibroblast. *BASEB J.* 1:398-402, 1987. [\[Context Link\]](#)
4. Chamberlain, G. J. Cyriax's friction massage: a review. *J. Orthop Sports Phys. Ther.* 4:16-21, 1982. [IUCAT Link](#) [A-to-Z Link](#) [Bibliographic Links](#) [\[Context Link\]](#)
5. Clark, R. A., J. Quinn, H. Winn, J. Lanigan, P. Dellepella, and R. Colvin. Fibronectin is produced by blood vessels in response to injury. *J. Exp. Med.* 156:646-651, 1982. [IUCAT Link](#) [A-to-Z Link](#) [Bibliographic Links](#) [\[Context Link\]](#)
6. Davies, P. and A. Allison. In: *Immunobiology of the Macrophage*. D. S. Nelson (Ed.). New York: Academic Press, 1976, pp 4427-4461. [\[Context Link\]](#)
7. Dyson, M. and J. Suckling. Stimulation of tissue repair by ultrasound: a survey of the mechanisms involved. *Physiotherapy* 64:105-108, 1978. [IUCAT Link](#) [A-to-Z Link](#) [Bibliographic Links](#) [\[Context Link\]](#)
8. Enwemeka, C. S. Connective tissue plasticity: Ultrastructural, biochemical, and morphological effects of physical factors on intact and regenerating tendons. *J. Orthop. Sports Phys. Ther.* 14:198-212, 1991. [IUCAT Link](#) [A-to-Z Link](#) [Bibliographic Links](#) [\[Context Link\]](#)
9. Enwemeka, C. S. Inflammation, cellularity, and fibrillogenesis in regenerating tendon: implications for tendon rehabilitation. *Phys. Ther.* 69:816-825, 1989. [\[Context Link\]](#)
10. Epstein, E. H., Jr. (Alpha1(3))3 human skin collagen. Released by pepsin digestion and preponderance in fetal life. *J. Clin. Invest.* 53:3225-3231, 1974. [\[Context Link\]](#)
11. Frieder, S., J. Weisberg, and B. Flemming, et al. A pilot study: the therapeutic effects of ultrasound following partial rupture of Achilles tendons in male rats. *J. Orthop Sports Phys. Ther.* 10:39-46, 1988. [IUCAT Link](#) [A-to-Z Link](#) [Bibliographic Links](#) [\[Context Link\]](#)
12. Gelbermann, G. H., P. Manske, J. Vandeberg, P. Lesker, and W. Akesson. Flexor tendon repair *in vitro*: a comparative histologic study of the rabbit, chicken, dog, and monkey. *J. Orthop. Res.* 2:39-48, 1984. [IUCAT Link](#) [A-to-Z Link](#) [Bibliographic Links](#) [\[Context Link\]](#)
13. Gross, M. T. Chronic Tendinitis: pathomechanics of injury factors affecting the healing response and treatment. *J. Orthop. Sports Phys. Ther* 16:248-61, 1992. [\[Context Link\]](#)
14. Harper, J., D. Amiel, and E. Harper. Collagenase production by rabbit ligaments and tendons. *Connective Tissue Res.* 17:253-259, 1988. [\[Context Link\]](#)
15. Hølund, B., I. Clemmensen, P. Junker, and H. Lyon. Fibronectin in experimental granulation tissue. *Acta Pathol. Microbiol. Immunol. Scand. (A)*90:159-165, 1982. [IUCAT Link](#) [A-to-Z Link](#) [Bibliographic Links](#) [\[Context Link\]](#)
16. Kurkinen, M., A. Vaheri, R. Roberts, and S. Stenman. Sequential appearance of fibronectin and collagen in experimental granulation tissue. *Lab. Invest.* 43:47, 1980. [IUCAT Link](#) [A-to-Z Link](#) [Bibliographic Links](#) [\[Context Link\]](#)
17. Leadbetter, W. B. Cell-matrix response in tendon injury. *Clin. Sports Med.* 11:533-77, 1992. [IUCAT Link](#) [A-to-Z Link](#) [Bibliographic Links](#) [\[Context Link\]](#)
18. Madden, J. W. and A. Arem. Wound healing: Biologic and clinical features. In: *Textbook of Surgery*, 14th Ed. D. C. Sabiston(Ed.). Philadelphia: W. B. Saunders, 1991. [\[Context Link\]](#)
19. McLeod, K. J., R. Lee, and H. Ehrlich. Frequency dependence of electrical field modulation of fibroblast protein synthesis. *Science* 236:1465-1469, 1987. [\[Context Link\]](#)
20. Nessler, J. P. and D. Mass. Direct-current electrical stimulation of tendon healing *in vitro*, *Clin. Orthop.* 217:303-312, 1987. [\[Context Link\]](#)
21. Norris, C. M. *Sports Injuries*. New York: Butterworth-Heinemann, 1993. [\[Context Link\]](#)
22. Nwachukwu, I. N. *Effect of Two Different Periods of Early Pulsed Ultrasound Application on the Tensile Strength of Ruptured Achilles Tendons In Rats*. Doctoral dissertation, New York University, 1985. [\[Context Link\]](#)
23. Owoeye, I., N. Spielholz, J. Fetto, and A. Nelson. Low-intensity pulsed galvanic current and the healing of tenotomized rat achilles tendons: preliminary report using load-to-breaking measurements. *Arch. Phys. Med. Rehabil.* 68:415-9, 1987. [IUCAT Link](#) [A-to-Z Link](#) [Bibliographic Links](#) [\[Context Link\]](#)

24. Prentice, W. E. *Therapeutic Modalities in Sports Medicine*. St. Louis: Times/Mirror/Mosby, 1990. [\[Context Link\]](#)
25. Salamon, A. and J. Harmori. Present state of tendon regeneration: light and electron microscopic studies of the regenerating tendon of the rat. *Acta Morphol. Hung.* 14:7-24, 1966. [\[Context Link\]](#)
26. Silver, I. A. and P. Rossdale. A clinical and experimental study of tendon injury, healing and treatment in the horse. *Equine Vet J.* (Suppl. 1):1-43, 1983. [IUCAT Link](#) [A-to-Z Link](#) [Bibliographic Links](#) [\[Context Link\]](#)
27. Williams, I. F. Studies on the pathogenesis of equine tendonitis following collagenase injury. *Res. Vet. Sci.* 36:326-338, 1984. [IUCAT Link](#) [A-to-Z Link](#) [Bibliographic Links](#) [\[Context Link\]](#)
28. Williams, I., K. McCullagh, and I. Silver. The distribution of types I and III collagen and fibronectin in the healing equine tendon. *Connect. Tissue Res.* 12:211-227, 1984. [IUCAT Link](#) [A-to-Z Link](#) [Bibliographic Links](#) [\[Context Link\]](#)
29. Zamora, A. J. and J. Marini. Tendon and myo-tendinous junction in an overloaded skeletal muscle of the rat. *Anat. Embryol.* 179:89-96, 1988. [IUCAT Link](#) [A-to-Z Link](#) [Bibliographic Links](#) [\[Context Link\]](#)

MASSAGE; PHYSICAL THERAPY; TENDINITIS; ACHILLES TENDON; FIBROBLASTS; INFLAMMATION; COLLAGEN; FIBRONECTIN

Accession Number: 00005768-199703000-00005

Copyright (c) 2000-2007 [Ovid Technologies, Inc.](#)

Version: rel10.5.1, SourceID 1.13281.2.21